

*Research Article***Determination of Thermal Behavior from Core Flux Density with Image Processing Technique for Distribution Transformers****Busra Aslan<sup>a,\*</sup> , Selami Balci<sup>b</sup> , Ahmet Kayabasi<sup>b</sup>** <sup>a</sup>*Karamanoglu Mehmetbey University, Graduate School of Natural and Applied Sciences, Department of Mechatronic Engineering, Karaman, Turkey*<sup>b</sup>*Karamanoglu Mehmetbey University, Faculty of Engineering, Department of Electrical and Electronics Engineering, Karaman, Turkey*

## ARTICLE INFO

## ABSTRACT

*Article history:*

Received 3 August 2024

Accepted 9 September 2024

*Keywords:*Fault diagnosis  
Flux distribution  
Image processing  
Thermal behavior  
Transformer

Considering the design and operating conditions of transformers, electromagnetic and mechanical stresses cause aging and negatively affect their operating performance. Advanced fault diagnosis methods have been developed based on information system-based remote online monitoring or electrical data obtained from sensors or sample windings added to the transformer core. The electromagnetic field distribution in the core structure of the transformer can respond quickly and effectively to fault situations. Therefore, changes in flux density within the core can be analyzed using image processing and/or data analysis methods. In this study, electromagnetic modeling of a distribution transformer with nominal values of 34.5/0.4 kV and 2000 kVA was conducted using Finite Element Analysis (FEA) software. Image processing techniques were applied to observe the behavior of the flux distributions on the core when the transformer was under nominal sinusoidal voltage. Then, considering the effect of the flux distribution in the core on the thermal state of the transformer, the thermal behavior of the core was derived with mathematical equations and shown on the transformer. Thus, the flux distribution in the core of a distribution transformer operating under nominal power conditions was examined and, a novel approach based on simulation studies was proposed to determine the flux distributions and thermal behavior of the transformer under fault conditions.

This is an open access article under the CC BY-SA 4.0 license.  
(<https://creativecommons.org/licenses/by-sa/4.0/>)

**1. Introduction**

In recent years, the performance of transformers in terms of their electromagnetic and mechanical effects and nonlinear behavior depending on operating conditions has become a subject that requires further study. While these studies are possible experimentally on the material or with remote monitoring, they can also be carried out with electromagnetic modeling-based software such as Finite Element Analysis (FEA), which allows simulation studies of operating conditions during the R&D process [1]. Electrical power losses occurring in the core and windings may vary depending on operating conditions. The operating conditions of transformers can generally be described as distortions in flux distribution due to insulation problems in the windings, extra power losses due to leakage flux behavior at the core junctions, and power losses due to harmonic components

resulting from their increased exposure to non-linear current loads in recent years. Mechanically, there may be vibration effects, temperature behavior, and cooling systems performance analysis, which directly affect the lifespan of the transformer. Vibration effects and temperature increases are important issues to consider as they accelerate the aging of insulation materials [2, 3]. Examples of past literature on these topics are summarized below.

In general, electrical faults that occur due to insulation deterioration between the windings on the high-voltage side greatly affect the operating performance of the transformer. Hajiaghahi, et al. [4] examined in detail the leakage flux effects occurring in the transformer core for fault detection between the windings. Thus, by considering methods based on flux leakage, they also evaluated the location, severity, load power factor and loading effects of the transformer in

\* Corresponding author. E-mail address: [busraaslan@kmu.edu.tr](mailto:busraaslan@kmu.edu.tr)  
DOI: 10.58190/ijamec.2024.105

the process of detecting faults between the windings. As a result of these evaluations, they developed two online methods based on leakage flux and vibration analysis. In the first method, they analyzed the voltage values induced in the sample windings to detect the fault occurring in the transformer windings. In the second method, they measured the vibration of the transformer with a digital accelerometer sensor and compared two different vibration datasets for the faulty and non-faulty cases, and then performed the fault detection by taking into account the amount of difference between the reference values in the non-faulty state. In order to determine the accuracy of their proposed method, they conducted experiments on a distribution transformer rated at 20/0.4 kV, 50 kVA rated values and compared them with simulation results. As a result, they stated that methods for detecting transformer faults based on leakage flux values can be used with high accuracy.

Insulation deterioration occurring in transformer windings may cause the magnetic leakage flux distribution to change [5]. Remote online monitoring of magnetic flux changes is very important in preventing any faults in transformers before they occur. However, to detect transformer faults using this method, the magnetic flux distribution in the core must be known under many operating conditions. Ouyang, et al. [6] carried out simulation studies for different winding faults of a 35 kV power transformer. With these simulation studies, abnormal operating conditions, including DC component effects and external short circuit faults, were examined. As a result, it was determined that the leakage fluxes caused by different winding faults in transformers vary from one another. Additionally, the magnetic flux distribution within the core can be effectively utilized for diagnosing transformer faults and estimating fault locations.

Winding faults occurring in transformers cannot be detected by traditional protective relays because they cause a small change in terminal currents and voltages. Mostafaei and Haghjoo [7] developed a technique based on the flux distribution in the core at nominal conditions in a non-faulty state, in order to detect winding faults occurring in power transformers. To determine the nominal flux distribution in the core, search coils were placed on the core legs and these coils were designed with multiple windings. Thus, under normal operating conditions, equal voltages were induced in the search coils due to equal (homogeneous flux distribution) flux passing through the transformer core parts (yoke and legs). However, if the voltage induced in any search coil differed from the nominal values, it was concluded that there was a fault in the transformer. A real 50 kVA, 20 kV/400 V three-phase distribution transformer was used to test the proposed method, and the proposed method was reported to work accurately in identifying transformer winding faults.

Power transformers are exposed to a lot of electrical, mechanical and thermal stress during their operation. These pressures cause insulation failures, called aging, in transformers. Insulation faults can cause great damage to

both the transformer and the grid in terms of power quality, and these bad effects cause huge costs [8]. For this reason, many studies have targeted approaches focused on early detection of transformer faults. In most of these approaches, a remote online monitoring method of power transformers that can be used experimentally is recommended. Cabanas, et al. [8] proposed to monitor the leakage flux behavior of the transformer online. For this purpose, they used an industrial power transformer with 400 kVA-20 kV rated values and measured the leakage flux of the transformer easily and inexpensively in faulty and non-faulty states, thanks to simple sensors. Then, they discussed the results obtained from these measurements and emphasized that their proposed method for measuring leakage flux behavior based on fault diagnosis works with high performance. A similar study to Cabanas, et al. [8] was also conducted by Athikessavan, et al. [9]. In that study, they presented a new technique for detecting inter-winding faults of dry-type transformers. In the presented method, they examined the online operating conditions of the transformer. In this method, they measured the leakage fluxes on the outer parts of the transformer using two flux sensors. Then, to test the accuracy of this proposed method, theoretical analyzes were carried out at different fault sizes and experimental tests were carried out on a transformer with a power rating of 10 kVA. Additionally, a factory-made device that monitors the healthy condition of the transformer was used to evaluate/compare the test results. Thus, it was seen that the results obtained in both cases were in agreement.

Today, with the development of imaging tools and the use of image processing techniques, many faults that can endanger human life can be detected during the maintenance of transformers. Vidhya, et al. [10] obtained images using a thermal camera to observe the change in temperature distribution in and around transformer ventilation pipes. Then, they applied the Symlet wavelet transform to these images. After the transformation, the state of the transformer was easily observed by examining the parameters of the image at various decomposition levels. Various images obtained from decomposition clearly revealed the temperature changes in the ventilation pipes of the transformer under different operating conditions. The obtained images were compared with normal operating parameters and it was observed that there were large differences between the faulty state parameters.

In general, thermal models are used to predict thermal behavior, hot spots and faults in transformers [12]. Shiravand, et al. [11] used a new thermal model, thermography, and fluid dynamics methods to obtain transformer oil and radiator temperature. In the model, they took into account the thermal behavior of the environment where the transformer is located, the oil in the boiler, the windings and the radiator. They modeled the heat transfer between these environments with nonlinear thermal resistances. They used three distribution transformers to test

the accuracy of their proposed method. They emphasized that the method they proposed was quite successful, according to the experimental results. In the study, they used a thermal camera to take thermal images and image processing techniques to analyze them. Using the thermal images obtained, they determined the temperature of the transformer oil and the radiator temperature. At the end of the study, they suggested that faults occurring in the transformer cooling system could be easily detected by using the thermal modeling they developed.

In the event of power transformer failures, the location and type of failure must be determined accurately and quickly. For this purpose, Fang, et al. [12] proposed a technique based on infrared image processing techniques and semi-supervised learning methods for transformer fault detection. In their study, they first extracted temperature, texture and shape features from infrared image data as model reference vectors. They then created a Generative Adversarial Network (GAN) to obtain synthetic data in addition to labeled features. In addition to traditional supervised learning methods, the method was able to learn information from unlabeled sample data. Finally, a dataset was obtained from a company in China to test their proposed method. As a result, they demonstrated that transformer fault classification can be made accurately with the proposed method.

As can be understood from the above paragraphs, fault detection and thermal analysis remain an active research area. This study focuses on analyzing the thermal behavior of the transformer based on flux density. In this context, electromagnetic modeling of the power distribution transformer with 2000 kVA power and 34.5/0.4 kV voltage ratios was performed with FEA software. The flux distributions in the core were analyzed and flux extractions were conducted using image processing techniques. Thus, the flux distributions in the core of a power distribution transformer under nominal operating conditions were extracted and it became possible to visually analyze the electromagnetic effects of the core behavior on the flux distribution in fault situations. Subsequently, the effect of changing flux distribution in the core on the core temperature behavior in different fault situations was examined. Using image processing techniques, thermal images related to the flux distribution images of the core were extracted and the results obtained in the study were discussed comparatively.

The study contributes significantly to the existing literature on transformer fault detection by proposing an image processing-based approach to analyze the flux distribution and its relationship with the thermal behavior of transformer cores. The use of FEA for modeling flux distribution under different fault conditions (healthy, short circuit, and voltage imbalance) adds a new dimension to fault diagnosis techniques. The study provides a visual analysis of flux distributions, which is unique in this field, allowing for better understanding and early detection of issues related to transformer windings and operating conditions. Moreover,

the proposed method enhances the detection of potential faults by converting flux distribution data into thermal behavior images, helping to predict overheating and other issues that could cause transformer failure.

Compared to existing methods such as vibration-based fault detection and search coil-based techniques, this study's approach offers a more precise and automated way of detecting faults through image processing techniques. Unlike traditional methods that rely on physical measurements or sensor data, this study integrates electromagnetic modeling and image processing to derive thermal behavior, which can lead to more accurate and faster fault detection. By creating a comprehensive dataset of images based on FEA simulations and applying multi-level thresholding techniques, the study moves beyond sensor-based approaches, offering a highly efficient, non-intrusive solution for continuous monitoring and analysis of transformer conditions.

The study focuses on determining the thermal behavior of transformers using flux density and image processing techniques. It contributes to the literature by integrating FEA with advanced image processing methods to model electromagnetic fields and derive thermal states under varying fault conditions. This work builds upon previous studies that have investigated fault detection in transformers using leakage flux and electromagnetic modeling. Recent advances in transformer fault detection have introduced various techniques that integrate flux analysis, image processing, and machine learning. For example, the work by Hajiaghasi, et al. [13] utilized leakage flux and vibration analysis for fault detection in transformer windings, demonstrating the effectiveness of flux-based diagnostics under different fault conditions. Similarly, Ouyang, et al. [6] applied magnetics flux leakage to simulate and diagnose winding faults under different operational conditions. Both of these studies rely on flux distribution, which is also central to the current study, where flux behavior is analyzed to derive the thermal state of the transformer using image processing. However, unlike these studies, our work uniquely combines FEA with image processing to directly link flux distributions to thermal behavior in fault conditions, allowing for a visual representation of both electromagnetic and thermal dynamics. While Mostafaei and Haghjoo [14] and Athikessavan, et al. [9] used flux sensors and search coils to detect abnormalities, their methods lack the thermal analysis dimension that this study incorporates. Cabanas, et al. [8] and Vidhya, et al. [10] focused on online monitoring and wavelet transformation of thermal images, which are akin to the image-based approach here but do not integrate FEA modeling for flux-to-thermal conversion. Finally, Shiravand, et al. [15] utilized thermography and fluid dynamics for predicting cooling system faults, providing a thermal perspective similar to the current study but without the detailed electromagnetic modeling. This study's novel contribution lies in its ability to extract and analyze flux

distributions and corresponding thermal states simultaneously, offering a comprehensive method for fault detection in transformers. In summary, the proposed approach provides the following scientific contributions to the literature:

- Extraction of the flux density to temperature through image processing,
- Creating a dataset of images based on transformer FEA modelling and simulation,
- Obtaining the temperature behavior of the transformer core from flux distributions using image processing technique.

## 2. Electromagnetic Fundamentals of Transformers

The basic operating principle of transformers is based on the induction principle. Transformers, whose basic structure is given in Figure 1, consist of a magnetic core and windings around the core. The operation of the transformer is generally explained by Maxwell's Faraday and Ampere equations. Equation 1 shows Faraday's law, which explains how time-varying magnetic fields create electric fields, Equation 2 shows Ampere's law, which explains that the source of the magnetic field is electric current and time-varying electric field, Equation 3 shows Gauss's law, and Equation 4 shows Gauss's law for magnetism [16].

$$\nabla \times E = -\mu \frac{\partial H}{\partial t} \tag{1}$$

$$\nabla \times H = J + \frac{\partial E}{\partial t} \tag{2}$$

$$\nabla \cdot D = \rho_0 \tag{3}$$

$$\nabla \cdot E = 0 \tag{4}$$

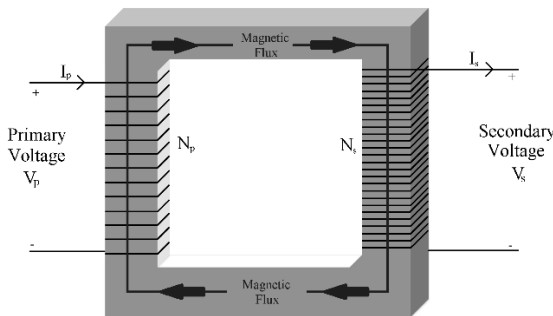


Figure 1. Structure and operating principle of the transformer

When  $V_p$  voltage is applied to the primary winding, time-varying flux begins to flow through the transformer according to Faraday's law. The core structure of the transformer has a greater permeability than the air in the external environment. Therefore, while most of the flux

passes through the transformer core, a very small part of it spreads to the environment. The flux that spreads to the environment is called stray flux or stray flux. As the time-varying flux passes through the secondary winding, a time-varying voltage  $V_s$  is induced in the secondary winding.

Unlike transformers manufactured in practice, the structure of the windings and core in an ideal transformer is perfect. Therefore, there is no loss. Since the permeability of the perfectly structured core is very high, no leakage flux occurs. In addition, in ideal transformers, the resistivity in the conductors is zero, so no voltage drop occurs. In practice, ideal transformer production is not possible. Therefore, leakage fluxes and physical properties of the windings should be taken into consideration when electromagnetic modeling of transformers [17].

### 2.1. Transformer Power Losses

Since there is no power loss in ideal transformers, the power values in the primary and secondary windings are equal. However, in practice, many losses occur due to the environmental and structural characteristics of transformers. The power relationship between the primary and secondary winding is given in Equation 5. ( $P_1$ : **primary winding**,  $S_2$ : **secondary winding**)

$$Power P1 = Power loss + Power S2 \tag{5}$$

Transformer losses can be divided into two categories as loaded and no-load losses depending on the load condition, and core and winding losses can be divided into two categories according to their place of occurrence. Since transformers do not have any moving parts, mechanical losses do not occur. However, operating transformers under non-ideal loads also causes losses. Transformer losses are shown with a block diagram in Figure 2 [18].

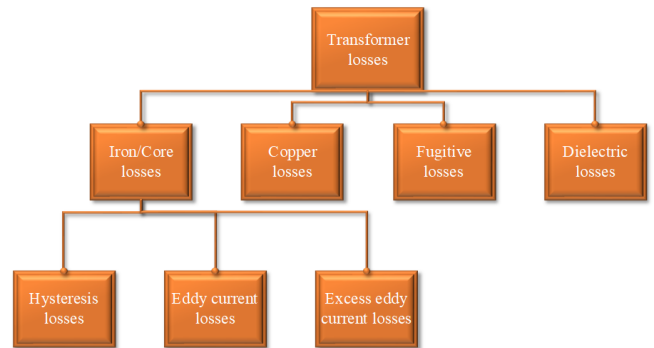


Figure 2. Transformer power losses

Iron losses: These power losses occurring in the transformer core are also called core losses. The reason for this loss is the magnetic flux occurring in the core. Iron losses are equal to the sum of eddy current losses and hysteresis losses.

Copper losses: Power losses of transformers due to ohmic resistance are called copper losses. Copper losses ( $P_c$ ) are expressed in Equation 6 [19].

$$P_c = I_1^2 R_1 + I_2^2 R_2 \quad (6)$$

Leakage Losses: Power losses caused by leakage field are called leakage losses. They can be neglected because they are very small compared to iron and copper losses.

Dielectric Loss: The losses occurring in the insulating materials of the transformer are called dielectric losses.

Hysteresis Loss: Friction of magnetic fields in the core lamination create hysteresis losses. Hysteresis losses constitute 50% to 80% of the no-load running-in losses in transformers. They vary depending on the characteristics of the transformer core material. For example, the hysteresis losses of a transformer core with amorphous steel material are less than those of a transformer core with a normal core. Hysteresis losses ( $P_h$ ) occur in the form of heat as given in Equation 7 [18, 19].

$$P_h = K_h B_{Max}^{1.6} f v \text{ (Watt)} \quad (7)$$

Eddy Current Losses: The current generated by the voltage applied to the primary winding of the transformer produces a time-varying magnetization flux in the transformer core. This flux induces a voltage in the secondary winding and current flows through the circuit at the secondary winding end. Alternating flux also induces Electromotive Force (EMF) in the transformer core. EMF causing current to flow locally in the transformer core. This current, which does not contribute to the transformer output, is released as heat. Eddy current losses ( $P_e$ ) are given in Equation 8 [19]. Eddy current losses in the windings is numerically estimated by precisely determining the peak leakage flux density in the gap between the primary and secondary windings [20].

$$P_e = K_e B_m^2 s^2 f^2 V \text{ (Watt)} \quad (8)$$

## 2.2. Flux Density and Fault Relationship in Transformers

Magnetic flux density ( $B$ ) is a very important parameter in transformers. It represents the force acting per unit current per unit length on a wire placed at right angles to a magnetic field. In other words, it measures how densely magnetic field lines pass through a particular area. The flux density depends on the magnitude of the current, its frequency and the core properties. The flux density in a transformer refers to the magnetic field strength in its core. It is a critical parameter that affects the performance and behavior of the transformer. The relationship between magnetic flux density ( $B$ ) and magnetic field density ( $H$ ) is expressed by Equation 9 [21, 22].

$$B = \mu H \quad (9)$$

Excessive flux may occur in transformers due to increase in voltage or decrease in frequency, and the flux density significantly affects the core area. High flux density leads to increased hysteresis and eddy current losses. Overheating, mechanical stresses or insulation failure in the core can be hazardous to the magnetic circuit. This can result in reduced efficiency, increased losses, and potential hot spots within the transformer. Therefore, there is a relationship between flux density, transformer losses, and faults. Flux density causes losses, which in turn cause localized heating and ultimately cause faults. At the same time, faults in the transformer may affect the flux density, altering the leakage flux distribution. This changes the leakage flux distribution. As a result, monitoring flux density changes is very important for fault detection [23-25].

Leakage flux-based methods are used in the literature for fault detection. These include vibration-based methods and search coil-based methods. In vibration-based methods, transformer vibrations are measured and compared with the normal situation to detect faults. In search coil-based methods, the voltage between the search coils is analyzed to detect leakage flux. These techniques are useful in detecting abnormalities in transformer windings, and experimental results in previous studies summarized in the introduction have demonstrated their effectiveness [13, 26, 27].

Detection of faults in transformers based on flux density changes is a research area. In this way, faults can be detected quickly, maintenance plans can be made accordingly, and early warning systems can be developed.

## 2.3. FEA Simulation

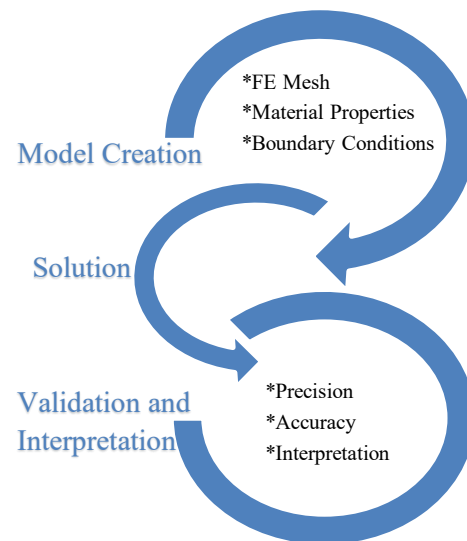


Figure 3. Block diagram of the FEA method

FEA was developed between 1941 and 1942 by Russian-Canadian Alexander Pavlovich Hrennikoff and German-American mathematician Richard Courant. Since its development, FEA has become widespread and is still frequently used today. In this way, very difficult

mathematical problems can be solved easily and consistently. The finite element method solves physical problems using partial differential equations. In this study, the transformer shown in Figure 4 was designed by following the steps in the block diagram given in Figure 3. The transformer core exhibits non-linear behavior. Therefore, the leakage flux distribution of the transformer cannot be determined by mathematical calculations. In this context, it is easier to achieve more realistic results by 3D electromagnetic modeling of the transformer using ANSYS Maxwell software. The characteristics of the transformer designed using ANSYS Maxwell software are given in Table 1.

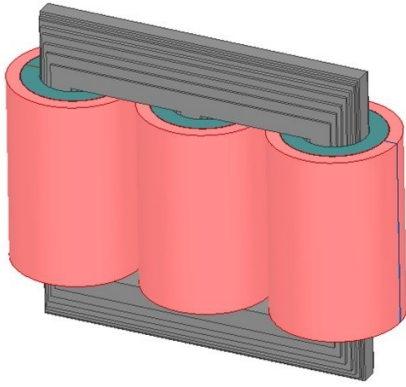


Figure 4. Transformer FEA modelling.

Table 1. Technical specs of a distribution transformer for FEA modelling.

Rated Power	2000 kVA
Operational Frequency	50 Hz
Rated Voltage	33/0.4 kV
Connection Type	Delta/Star (Dyn-0)
Core Material	SiFe (M4) 0.27 mm
Core Stacking Factor	0.96
Hysteresis Coefficient ( $K_h$ )	46.206
Eddy Current Coefficient ( $K_e$ )	0.2902
Mass Density	7650 kg/m <sup>3</sup>
Conductivity	1960000 S/m
Primary Winding	1942 turns / AWG copper
Secondary Winding	13 turns / Aluminum foil
No-load Losses (Core Losses)	3.2 kW
Full-load Losses (Winding Losses)	21 kW
Full-Load Efficiency	%98.8
Cooling Type	ONAF (Oil Natural Air Forced)
Core Volume	0.218 m <sup>3</sup>
Winding Volume	0.155 m <sup>3</sup>

### 3. Dataset and Simulation Conditions

We conducted simulations using a 34.5/0.4 kV, 2000 kVA power distribution transformer model in ANSYS Maxwell. The transformer was simulated under nominal operating conditions as well as under short circuit and voltage imbalance scenarios. The parameters chosen for the simulations, such as material properties, operating frequencies, and boundary conditions, were based on standard transformer designs and real-world operational conditions. The transformer core material was set to SiFe (M4), with the primary winding made of AWG copper and the secondary winding made of aluminum foil. These conditions reflect typical operating environments for industrial transformers, allowing us to model realistic flux distribution patterns.

The dataset for the simulation was selected based on common fault scenarios in power distribution transformers, including healthy operation, short circuits, and voltage imbalances. These scenarios were chosen to cover a range of potential operational failures, allowing for a comprehensive analysis of how flux distribution patterns change under different conditions. Each scenario was simulated under the same environmental conditions to ensure that the results were directly comparable.

### 4. Image Processing-Based Extraction of Flux Distribution

Image processing covers all kinds of mathematical operations performed on image pixels for the purpose of extracting useful information, improving image quality, providing meaningful inferences from a large number of images or videos, etc.[28] Thanks to processes such as color spaces, transformations, filtering, edge detection, morphology, and thresholding applied to images, many different applications such as object detection, object tracking, activity detection, license plate detection, medical diagnoses, remote sensing, security and defense industry have become applicable with image processing [29, 30].

Image segmentation is a fundamental operation in almost all applications involving computer vision and image processing. Generally, in applications aimed at image enhancement and meaning, images are divided into multiple segments and objects. In this way, the object to be focused on in the image comes to the fore and is separated from other background components. Because of its importance, many image segmentation algorithms such as thresholding, region-growing and watershed methods have been developed in the past literature [31]. Among various segmentation techniques available in the literature, thresholding-based segmentation is one of the most effective and simple approaches due to its lower computational cost and high efficiency. Therefore, image thresholding is one of the most used techniques to perform image segmentation [32]. With image thresholding, an appropriate threshold value is selected that separates the foreground from the background, and pixels below this value are segmented as background, and pixels above this value are segmented as foreground. Determining the threshold value is

an important problem [33]. The Otsu method [34], which enables automatic adjustment of the threshold value, is one of the most successful threshold determination techniques that selects a global threshold value by maximizing the separability of pixels in gray space images. After the Otsu algorithm, the image turns into a two-class or binary image (or pixels above the threshold value and pixels below the threshold value). With the Otsu algorithm, the threshold value that minimizes the intra-class variance and maximizes the inter-class variance is found [35, 36]. Using the Otsu method, information in the image histogram is used to determine the light intensity in the image and select a threshold value accordingly. Assuming that an image is represented at gray level  $L$ , the  $L$  value for this image is a maximum of 255. If it is assumed that  $t$  represents the threshold value, the histogram is divided into  $w_1$  and  $w_2$  classes. This distinction can be expressed by the following equations. In Equation 10,  $p_i$  shows the probability of each pixel according to its gray level value.  $N$  refers to the total number of pixels.  $n_i$  indicates the number of pixels at each level  $i$ . According to the determined  $t$  value, pixels are divided into two classes: those below the  $t$  value and those above the  $t$  value. The probability distributions for these two classes are as in Equation 11 and Equation 12. To calculate the variance between classes, class averages are found as in Equation 13 and Equation 14. Equation 15 shows the inter-class variance ( $\sigma$ ).  $u_T$  gray level is the total average of gray level pixels. Equation 16 is the within-class variance equation. With these variance equations, the optimal  $t$  value that minimizes the intra-class variance and maximizes the inter-class variance is selected with Equation 17 [37].

$$p_i = n_i/N \quad (N = n_1 + n_2 + n_3 + \dots + n_L) \quad (10)$$

$$w_1 = \sum_{i=0}^t p_i \quad (11)$$

$$w_2 = \sum_{i=t+1}^L p_i \quad (12)$$

$$u_1 = \sum_{i=0}^t ip_i/w_1 \quad (13)$$

$$u_2 = \sum_{i=t+1}^L ip_i/w_2 \quad (14)$$

$$\sigma_B^2 = w_1(u_1 - u_T)^2 + w_2(u_2 - u_T)^2 \quad (15)$$

$$(u_T = w_1u_1 + w_2u_2)$$

$$\sigma_W^2 = \sum_{i=1}^2 w_i/\sigma_i^2 \quad (16)$$

$$t = \arg\{\max(\sigma_B^2(t))\} = \arg\{\min(\sigma_W^2(t))\} \quad (17)$$

$$(0 \leq t \leq L)$$

$$t_1, t_2, t_3, \dots = \arg\{\max(\sigma_B^2(t_1, t_2, t_3, \dots))\} = \arg\{\min(\sigma_W^2(t_1, t_2, t_3, \dots))\} \quad (18)$$

$$(0 \leq t \leq L)$$

In applications where the image contains more than two classes or segments, the Otsu method is easily extended to multi-level thresholding [38]. Considering that the threshold values ( $t_1, t_2, t_3, \dots$ ) that divide the pixels in the image into  $w_1, w_2, w_3, \dots$  classes will be selected, Equation 12 can easily be converted to Equation 18. As can be understood, for multi-level thresholding, more than one threshold is determined and segmentation is applied to the image according to these threshold ranges [39].

In this application, image processing techniques were applied to transformer images with flux distribution in Tesla obtained through simulation from the ANSYS program. Transformer images showing the flux distribution in the transformer were obtained through the ANSYS program. The parameters used for the ANSYS simulation are shown in Table 1. The simulated transformer is designed in three different states: healthy, short circuit and voltage unbalanced. It is clearly seen in Figure 5 that the flux distributions are different for the three different cases. With the Otsu method and the Multilevel Otsu method explained between Equation 5 and Equation 13, the flux density in these images was determined, marked and a colorbar was created. Figure 5 shows the image processing steps applied to ANSYS images, respectively. First, the raw transformer images with flux distribution obtained as a result of the ANSYS program simulation were cropped so that only the transformer area remained. As seen in the cropped image, the effect created by the flux distributions is colored by the ANSYS program. The coloring in this process is generated based on the intensity variations of the flux distribution in the image. Since the flux distribution contains a wide range of values, it is essential to apply multi-level thresholding to effectively segment the image into distinct regions. Multi-level thresholding divides the image into multiple segments, where each segment corresponds to a range of flux intensity values, allowing for a clearer distinction between areas with different flux concentrations. To achieve this, the Otsu method is utilized, which is known for automatically determining optimal threshold values by minimizing the intra-class variance of pixel intensities. First, the cropped image is converted into a grayscale format, simplifying the flux data into intensity levels that can be more easily processed. This grayscale image is then subjected to multi-level thresholding. The number of thresholds, in this case, is set to 10, a value chosen based on the complexity and raw distribution of flux intensities in the original image.

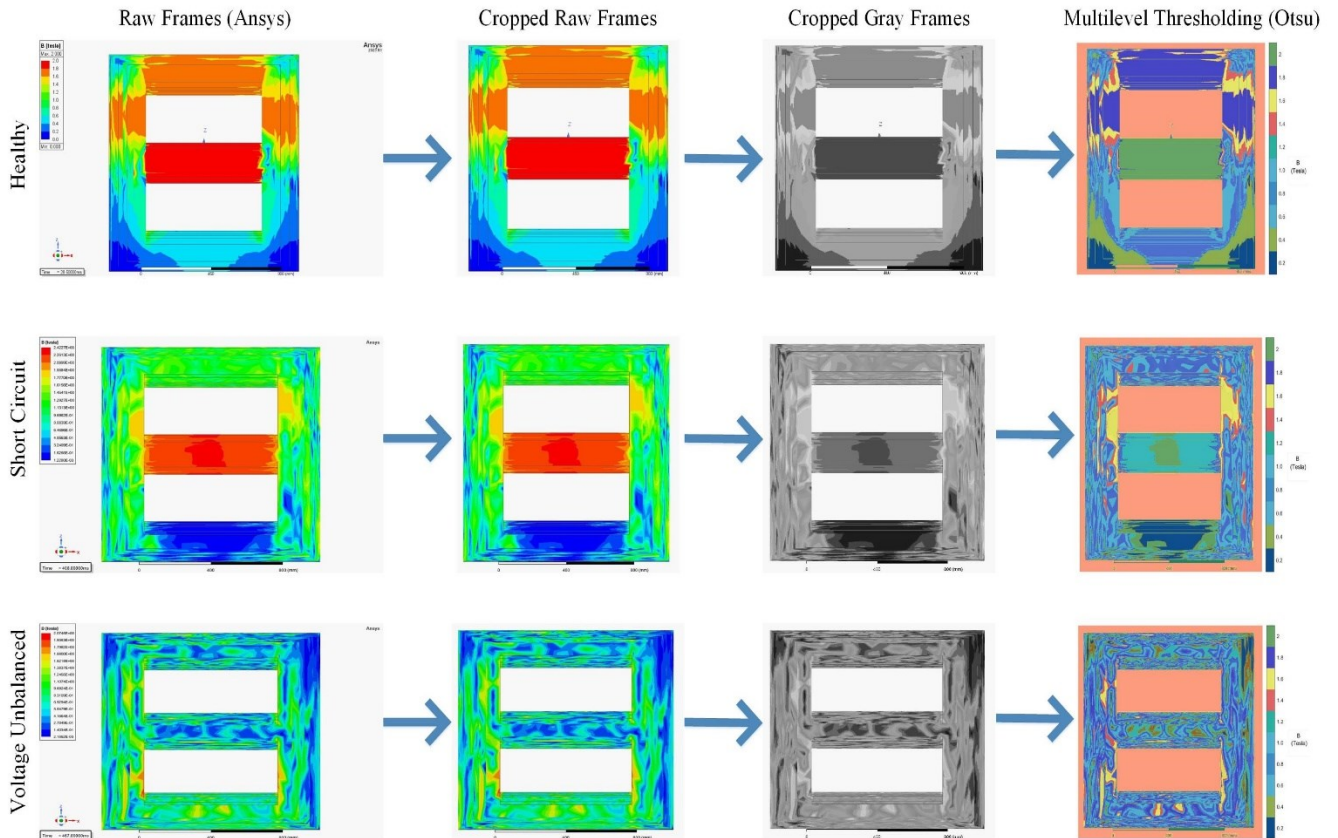


**Figure 5.** Steps for creating flux distribution with multilevel thresholding. (First, raw images are cropped. Then, these images are converted from RGB to gray space. Finally, multilevel thresholding is applied.)

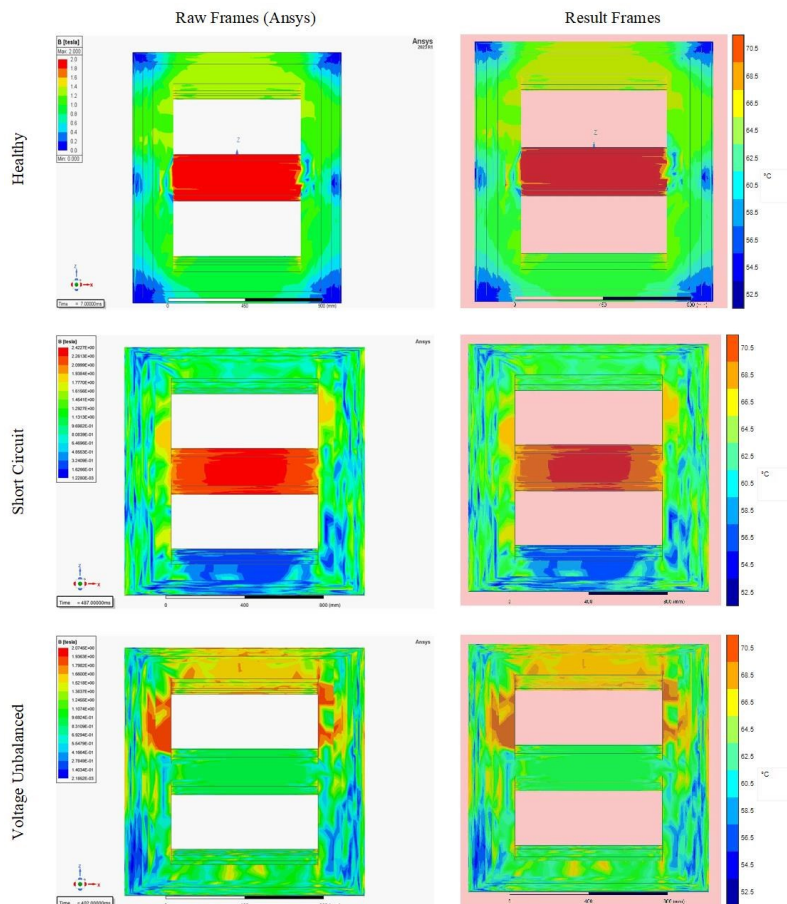


**Figure 6.** Creating thermal behavior based on flux distribution. (Using the flux distribution of the raw images on the left, the images on the right, i.e. the thermal behavior, are extracted.)

The 10 threshold values created through Otsu's method divide the image into 11 distinct regions, each corresponding to a different flux intensity range. These regions are then colored differently, with each color representing a specific range of flux values. This technique not only highlights the varying flux intensities but also enhances the visual interpretation of the distribution. By assigning unique colors to each thresholded region, it becomes easier to identify transitions in the flux, which are often crucial for analyzing phenomena like electromagnetic field distributions in transformers. Additionally, a color bar is included in the output image, serving as a reference that maps each color to its corresponding flux intensity value. In summary, this approach provides a comprehensive visualization of flux distribution by employing multi-level thresholding to segment and color the image, enhancing both interpretation and analysis of the transformer regions according to the flux intensity.

These image processing operations were performed in MATLAB, utilizing the Image Processing Toolbox for image analysis and processing tasks. The multi-level thresholding was executed using the *multithresh* function, which applies Otsu's method to automatically determine the optimal threshold values. Based on the threshold values obtained, the *imquantize* function was used to segment the image into different regions, and each region was colored using the *label2rgb* function to reflect different levels of flux intensity. Finally, a color bar was added to the result image to display the flux distribution values corresponding to the colors in the image.

## 5. Relationship Between Flux Distribution and Thermal Behavior of Transformer

As a result of the simulations carried out in the study, images of the flux distributions of different error situations in the transformer core were obtained. The relationship between the flux values in these images and the thermal state of the transformer was then derived using the formulas given in Equations 19-23. Finally, the thermal behavior of the transformer core was developed and presented with image processing techniques. Based on these equations, thermal temperature values were derived from the flux distributions for the transformer under three different conditions. In this context, new images showing thermal temperature distributions were created from the simulation images in the ANSYS program, which were obtained for healthy, short circuit, and voltage unbalanced situations. A sample of each situation is shown as an example in Figure 6.

$$B_v(T) = \frac{2hv^3}{c^2} \frac{1}{\exp\left(\frac{hv}{kT}\right) - 1} \quad (19)$$

$$B_{RJ}(v, T) = \frac{2v^2}{c^2} kT \quad (20)$$

$$T = \frac{\lambda^2}{2k} I_v \quad (21)$$

$$\frac{dv}{c} = \frac{dv}{v} \quad (22)$$

$$\int T dv = \frac{\lambda^3}{2k} \int I_v dv \quad (23)$$

## 6. Conclusion and Discussion

In this study, images of the behavior of the flux distribution in the core of a power transformer with a nominal value of 34.5/0.4 kV and 2000 kVA, which is frequently used in the grid power distribution system, were obtained using FEA electromagnetic modeling software under nominal loading and operating conditions. The flux distribution was created for three different states of the transformer: Healthy, short circuit and voltage unbalanced. It has been observed that the flux distributions are different depending on the fault condition. Subsequently, the flux distribution was extracted from these images with the multi-level thresholding technique, which is one of the image processing techniques. Unlike the previous literature, thanks to an approach to visually examine the flux distributions in the transformer core under nominal operating conditions, distortions in the flux distributions in different fault situations can also be analyzed. Thus, in nominal operating conditions, the proposed method can be used as an image processing-based approach to evaluate the flux distribution for determining whether there is a problem with the transformer windings or operating conditions. Additionally, after the flux distribution in the transformer core is extracted using the proposed approach, the relationship between the flux distribution and the thermal behavior of the transformer core is examined. By converting flux distributions into thermal temperature values, the thermal state of the transformer and therefore fault detection can be performed.

The results demonstrate that the proposed method is effective in visualizing the flux distribution and identifying thermal hot spots, particularly under fault conditions such as short circuits and voltage imbalances. The multi-level thresholding technique provided clear segmentation of flux intensity values, which were directly correlated with the transformer's thermal behavior. This method not only offers a reliable way to monitor flux distributions in real time but also allows for early fault detection by predicting potential overheating in the transformer core.

The limitations of this study include the lack of

experimental validation and the use of only one transformer model. To address these, future work should involve testing the method on a wider variety of transformer designs and operational conditions. Moreover, integrating real-time sensor data with the FEA simulations would improve the model's accuracy and make the method more applicable in industrial environments. Conducting additional experiments, such as real-time monitoring of transformers in the field, would provide a more comprehensive understanding of how flux distribution patterns and thermal behavior evolve over time in different scenarios.

In future studies, the robustness of the proposed methodology can be further strengthened by applying it to a wider range of transformer datasets with varying power ratings, operating conditions, and fault scenarios. By analyzing multiple datasets, the generalizability of the method will be demonstrated, and the effectiveness of flux distribution analysis under different transformer configurations will be validated. Moreover, conducting additional experimental tests, such as real-time monitoring of transformers in industrial environments, could provide a more comprehensive understanding of the method's applicability in practical settings. These steps will help ensure that the method remains reliable across diverse operational conditions.

Additionally, further research should focus on improving the accuracy of the mathematical models used to derive thermal behavior from flux density. The current models are based on certain assumptions and simplifications, such as uniform core material properties and idealized boundary conditions. Future work could explore more advanced modeling techniques that account for material heterogeneities, non-linear electromagnetic behavior, and real-world boundary effects. Integrating real-time data from sensors and developing adaptive models that learn from operational data could also enhance the accuracy and predictive power of the thermal analysis, making the method even more reliable for early fault detection.

Finally, in future studies, remotely recorded online thermal images will be processed using advanced image processing techniques to more accurately determine the thermal behavior of transformers. These images will enable real-time monitoring of transformers under various operational conditions, allowing for the early detection of anomalies that could lead to overheating. By continuously analyzing the thermal data, it will be possible to identify patterns or irregularities associated with emerging faults, such as insulation deterioration or cooling system malfunctions. This approach will facilitate the development of predictive maintenance strategies, reducing the risk of unexpected transformer failures and extending their operational lifespan.

## References

- [1] M. F. Unleresen, S. Balci, M. F. Aslan, and K. Sabanci, "The Speed Estimation via BiLSTM-Based Network of a BLDC Motor Drive for Fan Applications," *Arabian Journal for Science and Engineering*, vol. 47, no. 3, pp. 2639-2648, 2022/03/01 2022, doi: 10.1007/s13369-021-05700-w.
- [2] X. Duan, T. Zhao, J. Liu, L. Zhang, and L. Zou, "Analysis of Winding Vibration Characteristics of Power Transformers Based on the Finite-Element Method," *Energies*, vol. 11, no. 9, p. 2404, 2018. [Online]. Available: <https://www.mdpi.com/1996-1073/11/9/2404>.
- [3] B. A. Thango, J. A. Jordaan, and A. F. Nnachi, "Analysis of Stray Losses in Transformers using Finite Element Method Modelling," in *2021 IEEE PES/IAS PowerAfrica*, 23-27 Aug. 2021 2021, pp. 1-5, doi: 10.1109/PowerAfrica52236.2021.9543100.
- [4] S. Hajiaghahi, M. M. Hosseini Ahmadi, P. Goleij, and A. Salemnia, "Transformer inter-turn failure detection based on leakage flux and vibration analysis," *IET Electric Power Applications*, vol. 15, no. 8, pp. 998-1012, 2021.
- [5] G. Sakallı and H. Koyuncu, "Identification of asynchronous motor and transformer situations in thermal images by utilizing transfer learning-based deep learning architectures," *Measurement*, vol. 207, p. 112380, 2023.
- [6] X. Ouyang, Q. Zhou, Z. Luo, Q. Jiang, M. Chen, and Y. Li, "Analysis on the magnetic flux leakage distribution in the transformer under different winding deformation and typical working condition," in *2020 IEEE International Conference on High Voltage Engineering and Application (ICHVE)*, 6-10 Sept. 2020 2020, pp. 1-4, doi: 10.1109/ICHVE49031.2020.9279691.
- [7] [7] M. Mostafaei and F. Haghjoo, "Flux-based turn-to-turn fault protection for power transformers," *IET Generation, Transmission & Distribution*, vol. 10, no. 5, pp. 1154-1163, 2016.
- [8] M. F. Cabanas *et al.*, "Insulation fault diagnosis in high voltage power transformers by means of leakage flux analysis," *Progress In Electromagnetics Research*, vol. 114, pp. 211-234, 2011.
- [9] S. C. Athikessavan, E. Jeyasankar, S. S. Manohar, and S. K. Panda, "Inter-Turn Fault Detection of Dry-Type Transformers Using Core-Leakage Fluxes," *IEEE Transactions on Power Delivery*, vol. 34, no. 4, pp. 1230-1241, 2019, doi: 10.1109/TPWRD.2018.2878460.
- [10] R. Vidhya, P. V. Ranjan, and N. R. Shanker, "Transformer breather thermal image decomposition for fault diagnosis," in *2021 7th International Conference on Electrical Energy Systems (ICEES)*, 11-13 Feb. 2021 2021, pp. 448-453, doi: 10.1109/ICEES51510.2021.9383639.
- [11] V. Shiravand, J. Faiz, M. H. Samimi, and M. Mehrabi-Kermani, "Prediction of transformer fault in cooling system using combining advanced thermal model and thermography," *IET Generation, Transmission & Distribution*, vol. 15, no. 13, pp. 1972-1983, 2021.
- [12] J. Fang, F. Yang, R. Tong, Q. Yu, and X. Dai, "Fault diagnosis of electric transformers based on infrared image processing and semi-supervised learning," *Global Energy Interconnection*, vol. 4, no. 6, pp. 596-607, 2021/12/01/ 2021, doi: <https://doi.org/10.1016/j.gloi.2022.01.008>.
- [13] S. Hajiaghahi, M. M. Hosseini Ahmadi, P. Goleij, and A. Salemnia, "Transformer inter-turn failure detection based on leakage flux and vibration analysis," *IET Electric Power Applications*, vol. 15, no. 8, pp. 998-1012, 2021, doi: <https://doi.org/10.1049/elp2.12076>.
- [14] M. Mostafaei and F. Haghjoo, "Flux-based turn-to-turn fault protection for power transformers," *IET Generation, Transmission & Distribution*, vol. 10, no. 5, pp. 1154-1163, 2016, doi: <https://doi.org/10.1049/iet-gtd.2015.0738>.
- [15] V. Shiravand, J. Faiz, M. H. Samimi, and M. Mehrabi-Kermani, "Prediction of transformer fault in cooling system using combining advanced thermal model and thermography," *IET Generation, Transmission & Distribution*, vol. 15, no. 13, pp. 1972-1983, 2021, doi: <https://doi.org/10.1049/gtd2.12149>.
- [16] D. Li, B. Wang, and J. Feng, "Simulation Analysis of Power

- Transformer Internal Short Circuit for Magnetic Flux Leakage Distribution Feature Extraction," in *2023 CAA Symposium on Fault Detection, Supervision and Safety for Technical Processes (SAFEPROCESS)*, 2023: IEEE, pp. 1-5.
- [17] S. Mousavi, "Electromagnetic modelling of power transformers for study and mitigation of effects of GICs," KTH Royal Institute of Technology, 2015.
- [18] A. Ibatullayeva, "Power Transformers in Electrical Transmission and Distribution Grids," České vysoké učení technické v Praze. Vypočetní a informační centrum., 2017.
- [19] H. Alamry and A. Alyousef, "Electrical power transformer," ed, 2016.
- [20] O. Al-Dori, B. Şakar, and A. Dönük, "Comprehensive Analysis of Losses and Leakage Reactance of Distribution Transformers," *Arabian Journal for Science and Engineering*, vol. 47, no. 11, pp. 14163-14171, 2022/11/01 2022, doi: 10.1007/s13369-022-06680-1.
- [21] Y. Zhuang *et al.*, "Improving Current Transformer-Based Energy Extraction From AC Power Lines by Manipulating Magnetic Field," *IEEE Transactions on Industrial Electronics*, vol. 67, no. 11, pp. 9471-9479, 2020, doi: 10.1109/TIE.2019.2952795.
- [22] J. Winders, *Power transformers: principles and applications*. CrC Press, 2002.
- [23] P. Osinski and P. Witczak, "Analysis of Core Losses in Transformer Working at Static Var Compensator," *Energies*, vol. 16, no. 12, p. 4584, 2023. [Online]. Available: <https://www.mdpi.com/1996-1073/16/12/4584>.
- [24] A. J. Moses, "Comparison of transformer loss prediction from computed and measured flux density distribution," *IEEE Transactions on Magnetics*, vol. 34, no. 4, pp. 1186-1188, 1998, doi: 10.1109/20.706473.
- [25] B. Sudha, L. S. Praveen, and A. Vadde, "Classification of faults in distribution transformer using machine learning," *Materials Today: Proceedings*, vol. 58, pp. 616-622, 2022/01/01/ 2022, doi: <https://doi.org/10.1016/j.matpr.2022.04.514>.
- [26] F. Mekic, R. Girgis, and Z. Gajic, "Power transformer characteristics and their effects on protective relays," in *2007 60th Annual Conference for Protective Relay Engineers*, 2007: IEEE, pp. 455-466.
- [27] L. Li *et al.*, "Distributed Magnetic Flux Density on the Cross-Section of a Transformer Core," *Electronics*, vol. 8, no. 3, p. 297, 2019. [Online]. Available: <https://www.mdpi.com/2079-9292/8/3/297>.
- [28] M. F. Aslan, A. Durdu, and K. Sabancı, "Shopping Robot that make real time color tracking using image processing techniques," *International Journal of Applied Mathematics Electronics and Computers*, vol. 5, no. 3, pp. 62-66, 2017.
- [29] T. S. Huang, W. F. Schreiber, and O. J. Tretiak, "Image processing," *Proceedings of the IEEE*, vol. 59, no. 11, pp. 1586-1609, 1971, doi: 10.1109/PROC.1971.8491.
- [30] M. Sonka, V. Hlavac, and R. Boyle, *Image processing, analysis, and machine vision*. Cengage Learning, 2014.
- [31] S. Minaee, Y. Boykov, F. Porikli, A. Plaza, N. Kehtarnavaz, and D. Terzopoulos, "Image Segmentation Using Deep Learning: A Survey," *IEEE Transactions on Pattern Analysis and Machine Intelligence*, vol. 44, no. 7, pp. 3523-3542, 2022, doi: 10.1109/TPAMI.2021.3059968.
- [32] S. Pare, A. Kumar, G. K. Singh, and V. Bajaj, "Image Segmentation Using Multilevel Thresholding: A Research Review," *Iranian Journal of Science and Technology, Transactions of Electrical Engineering*, vol. 44, no. 1, pp. 1-29, 2020/03/01 2020, doi: 10.1007/s40998-019-00251-1.
- [33] S. S. Al-Amri and N. V. Kalyankar, "Image segmentation by using threshold techniques," *arXiv preprint arXiv:1005.4020*, 2010.
- [34] N. Otsu, "A threshold selection method from gray-level histograms," *IEEE transactions on systems, man, and cybernetics*, vol. 9, no. 1, pp. 62-66, 1979.
- [35] S. Zhu, X. Xia, Q. Zhang, and K. Belloulata, "An Image Segmentation Algorithm in Image Processing Based on Threshold Segmentation," in *2007 Third International IEEE Conference on Signal-Image Technologies and Internet-Based System*, 16-18 Dec. 2007 2007, pp. 673-678, doi: 10.1109/SITIS.2007.116.
- [36] D.-Y. Huang and C.-H. Wang, "Optimal multi-level thresholding using a two-stage Otsu optimization approach," *Pattern Recognition Letters*, vol. 30, no. 3, pp. 275-284, 2009/02/01/ 2009, doi: <https://doi.org/10.1016/j.patrec.2008.10.003>.
- [37] D. Liu and J. Yu, "Otsu Method and K-means," in *2009 Ninth International Conference on Hybrid Intelligent Systems*, 12-14 Aug. 2009 2009, vol. 1, pp. 344-349, doi: 10.1109/HIS.2009.74.
- [38] P.-S. Liao, T.-S. Chen, and P.-C. Chung, "A fast algorithm for multilevel thresholding," *J. Inf. Sci. Eng.*, vol. 17, no. 5, pp. 713-727, 2001.
- [39] S. Arora, J. Acharya, A. Verma, and P. K. Panigrahi, "Multilevel thresholding for image segmentation through a fast statistical recursive algorithm," *Pattern Recognition Letters*, vol. 29, no. 2, pp. 119-125, 2008.